Chapter 3.

Human microtumors generated in 3D: novel tools for integrated in situ studies of cellular immunotherapy

Human microtumors generated in 3D: novel tools for integrated in situ studies of cellular immunotherapy

Lothar Hambach, MD[1,2], Andreas Buser, MD[1], Marcel Vermeij[3], Nadine Pouw[1], Zohara Aghai[1], Theo van der Kwast, MD, PhD[3], Els Goulmy, PhD[1]

[1]Dept. of Immunohaematology and Blood Transfusion, Leiden University Medical Center, The Netherlands, [2]Dept of Hematology, Hemostasis, Oncology and Stem cell transplantation Hannover Medical School, Germany, [3]Dept. of Pathology, Erasmus Medical Center, Rotterdam, The Netherlands

Cellular immunotherapy targeting human tumor antigens is a promising strategy to treat solid tumors. Yet, clinical results of cellular immunotherapy are disappointing. Moreover, the currently available human in vitro tumor models are not designed to study the optimization of T-cell therapies of solid tumors. Here, we describe a novel assay for the multi-parametric in-situ analysis of therapeutic effects on individual human three-dimensional (3D) tumors. Tumors of several millimeter diameter were generated from human cancer cell lines of different tumor entities in a collagen type I microenvironment. Using a newly developed approach for the efficient morphological analysis of these tumors, we found that these in vitro tumors resembled many characteristics of the corresponding clinical cancers such as histological features, immunohistochemical staining patterns, distinct tumor growth compartments and heterogeneous protein expression. Moreover, we developed standardized protocols to assess the response to therapy with tumor antigen specific T-cells by determining T-cell infiltration and destruction of tumors and by monitoring soluble factors and tumor growth. Human tumors engineered in 3D collagen scaffolds are excellent in vitro surrogates for avascular tumor stages allowing integrated analyses of the anti-tumor efficacy of cancer specific immunotherapy in situ.

INTRODUCTION

The overall success of cancer immunotherapy with tumor antigen specific T-cells is still low (1). Particularly, the in situ interaction of human T-cells with the tumor cells is poorly understood since most pre-clinical studies rely on suspension cell assays determining the anti-tumor efficacy of T-cells by single parameters such as cytotoxicity and cytokine release. However, a central hallmark of clinical tumors is not reflected by these assays, namely three-dimensionality. Three-dimensional (3D) growth strongly affects the tumor response to cellular immunotherapy for the following reasons: First, 3D tumor growth represents a hurdle for tumor specific T-cells, since they need to infiltrate into the tumors in order to be effective (2-4). Thus, appropriate assays modeling the T-cell-tumor interaction require tumors large enough to allow tumor infiltration by T-cells. Second, the gene expression profile of 3D tumor cell cultures is strongly altered compared to tumor cells growing in 2D (5,6). This alteration typically results in down-regulation (7) and heterogeneity (8) of tumor-associated antigens (TAA), known as an important problem in clinical cancer immunotherapy (8-10). Third, spatially distinct tumor niches in 3D show heterogeneous dynamics in cell growth and death (e.g. outer proliferative versus inner necrotic tumor regions) (5). Previous studies already indicated a heterogeneous chemosensitivity of these different niches (11,12). Fourth, the polarity of tumor cells organized in 3D and cellular interactions with extracellular matrix (ECM) in 3D leads to differences in the intracellular signaling compared to tumor

cells growing in 2D (13-16). Thereby, 3D growth can increase apoptosis resistance of tumor cells (5,17,18) and impair their response to treatment.

The tumor spheroid model, i.e. non-adherently cultured tumor cell agglomerates, was a first 3D in vitro approach (5,19). However, many tumor cell lines fail to create spheroids (20). The addition of ECM as key regulator of the tissue phenotype facilitated the generation of microtumors. Thereby, 3D tumor foci in matrigel (21) or synthetic polylactide-co-glycolide scaffolds (22) can be reliably engineered in vitro. However, none of the models combines growth of individual human tumors and the possibility to assess multiple parameters of their response to T-cell treatment in one assay. Moreover, an efficient histological analysis of individual tumors is cumbersome due the small tumor size in these assays. Ideal in vitro assays to study cancer immunotherapy require individual 3D human tumors that 1) are large enough to facilitate studies on T-cell infiltration, 2) have defined properties (e.g. known presence or absence of the target antigens), 3) reflect the heterogeneity of the target antigen expression present in many clinical tumors, 4) resemble relevant morphological aspects of 3D clinical tumors, including their tumor growth patters and their heterogeneous growth niches, and 5) can be easily and individually analyzed for multiple parameters of their response to treatment. We applied a method previously published in the murine setting (23) to generate individual human solid tumors of several millimeter diameter in collagen type I scaffolds in vitro and to monitor their response to cellular immunotherapy over a period of 7 days. Using a newly developed approach for the efficient histological analysis of these tumors, we found that 3D tumors generated from various well defined human tumor cell lines resemble a series of histological features of the corresponding clinical cancers (24). These 3D tumors enabled us to study the anti-tumor efficacy of human CTLs directed against minor histocompatibility antigens (mHags). MHags are HLA-restricted polymorphic antigens capable of mediating strong immune-responses after allogeneic stem cell transplantation (25)**.**

In the current report, we describe a standardized approach to generate individual human solid tumors in vitro and to analyze their response to antigen-specific T-cells. We show the details of 1) our new approach to study the histology of tiny tumors of several millimeter diameter, 2) the morphological and immunohistochemical features of these tumors and 3) the multi-parametric assessment of the tumor response to cellular immunotherapy.

MATERIALS AND METHODS

Human cancer cell lines

The breast cancer cell lines MCF-7 (26) and MDA-MB-231 (27) (American Type Culture Collection, Rockville, USA), the melanoma cell line 518A2 (28) (kindly provided by Dr. P. Schrier, Leiden University Medical Center, The Netherlands) and the renal cell carcinoma (RCC) cell line BB65-RCC (provided by Dr. B. Van den Eynde, Ludwig Institute for Cancer Research, Brussels, Belgium) were cultured in 5% fetal calf serum (FCS) in Iscove's modified Dulbecco's medium (IMDM, Invitrogen Life Technologies, Breda, The Netherlands). All cell lines were genomically typed for the minor histocompatibility antigens (mHags) HA-1 and H-Y by allele specific PCR (29) and analyzed for HA-1 mRNA expression as described (30). Tumor cell lines were designated "HA-1^{+}", if positive for the immunogenic HA-1^{H} allele and for HA-1 mRNA.

Generation and culture of HA-1 and H-Y specific CTLs

MHag specific CTL lines were generated from peripheral blood mononuclear cells (PBMCs) of HLA-$A2^{+}$/HA-1^{-} healthy donors as described earlier (31) or were isolated from patients after allogeneic stem cell transplantation (32). mHag CTL clones were recovered by limiting dilution of the mHag CTL lines. Approval was obtained from the Leiden University Medical Centre review board and informed consent was provided according to the Declaration of Helsinki.

Microtumor model

Microtumors in collagen matrix were generated according to a modified protocol described earlier (23). A base layer of 50 µl rat tail collagen (BD Biosciences Europe, Erembodegem, Belgium; 1.75 mg/ml in PBS according to the instructions of the manufacturer) was added to a 96-well flat bottom culture plate well and incubated at 37°C for 2h with closed lid. After 2h, a cancer cell agglomerate of $6x10^{4}$ tumor cells in 0.6 µl collagen (3.65 mg/ml) was placed on the base layer with a micropipette (Eppendorf Reference for 0.5-10 µl, Hamburg, Germany) with round tips (Sorenson Bioscience, Miniflex Round Tips 0.1-10 µl, Salt Lake City, Utah, USA). After incubation at 37°C for 45 minutes with slightly opened lid and additional 15 minutes without lid in the flow cabinet, a top layer of 50 µl collagen (1.31 mg/ml) was gently added. After incubation at 37°C for 30 minutes with closed lid 100 µl of 20% pooled human serum (HS) in IMDM was added. This procedure resulted in 1 microtumor per well. After 1 day, microtumors of comparable size and shape were selected for further analysis and equally distributed to the various treatment groups. Microtumors were treated with CTLs in 100 µl 20% HS in IMDM supplemented with 40 Cetus U/ml interleukin-2 (Chiron, Amsterdam, The Netherlands) or medium only. Microtumor growth was photographically documented on subsequent days with an inverted microscope (Axiovert 25, Zeiss, Jena, Germany). Two-dimensional microtumor area π*r1*r2 was calculated after determination of the 2 maximal orthogonal microtumor radii r1 and r2 (AxioVision 40 LE Version 4.5, Sliedrecht, The Netherlands) in these photographs.

Histology of microtumors

Microtumors in collagen type I were fixed with 4% formalin for 24h at 4ºC. Subsequently, microtumor containing collagen clots were detached from the well wall with a watchmakers forceps and transferred to a tissue to drain off excess formalin. The shape of the collagen clot changed upon transfer from a cylindrical to a round shape and upon fluid removal from a round to a bell shape. When there was no

further shrinkage anymore, the collagen clot was transferred into a metal tissue mold heated on a hot plate filled with 2% liquefied agar (agar select, Sigma, Zwijndrecht, Netherlands) at 65°C. After solidification at room temperature (RT), the microtumor containing agar block was removed from the tissue mold with a small spatula. The agar block was placed on a dark background so that the microtumor was visible as white nodule under a stereo dissecting microscope (Leica MZ 7.5, Rijswijk, The Netherlands). The agar block was dissected along the microtumor border and laterally trimmed with a scalpel. The microtumor containing segment was flipped into upright position and up to 3 agar segments with microtumors treated under the same condition were embedded into new liquid 2% agar at 65°C in a perpendicular way and with the microtumor cutting to the bottom. After solidification at RT, the agar block was removed from the tissue mold, placed into a tissue cassette, processed in a tissue processor and embedded in paraffin with the microtumor cutting edge on the bottom. This ensured that serial sectioning started directly at the microtumor border. Paraffin embedded material was sectioned at 4 µm with 100 µm interval. Sections were stained with Hematoxylin and eosin (H&E). Gomorri silver staining of reticulin was performed as described (33). Analysis was independently performed by two pathologists.

Immunohistochemistry

Deparaffinized and rehydrated slides were not pretreated (for S100 stain) or pretreated with microwave for 20 min in EDTA 1 mM, pH 8.0 (CD8) or with Tris-EDTA-buffer, pH 9.0 (all other antibodies). After washing 3x with 1% Tween in PBS and incubation with 0.5% Protifar (Protifar Nutricia Cuji, The Netherlands) blocking solution in 1% Tween in PBS for 30 min, slides were stained overnight at 4ºC: with antibodies against CD8 (clone 4B11, dilution 1/20, Novocastra, UK), pankeratin (clone AE1/AE3, dilution 1/200, Neomarkers, CA), EMA (clone E29, dilution 1/500, DAKO, Haverlee, Belgium), Vimentin (clone V9, 1/50, DAKO), CD10 (clone 5bc6, dilution 1/20, Monosan, Uden, The Netherlands), gp100 (clone HMB45, dilution 1/100, DAKO), Melan A (clone A103, dilution 1/200, Neomarkers), Estrogen receptor (clone 1D5, dilution 1/10, DAKO), S100 (1/400, DAKO), Ki-67 (clone MIB-1, dilution 1:100, DAKO). After washing 3x with 1% Tween in PBS, primary antibodies were detected with DAKO Envision Peroxidase/DAB kit according to the instructions of the manufacturer (DAKO, Heverlee, The Netherlands). Sections were counterstained with Mayer hematoxylin.

Quantification of IFN-γ release

IFN-γ concentration in the supernatant was determined with the Pelikline ELISA kit (CLB, Amsterdam, The Netherlands). Detection limit was 2 pg/mL.

RESULTS

Generation of microtumors and histological analysis

3D microtumors were generated from tumor cell lines by embedding tumor cell agglomerates between two layers of collagen type I on day 0 (Figure 1A, Materials and Methods). Collagen type I was selected as scaffold for tumor growth because of its capability to facilitate the generation of complex morphologies in vitro (34,35) and its high optical transparency allowing photographic documentation of microtumors in culture. Histological analysis of microtumors was performed after processing and paraffin-embedding according to a newly developed technique. This methodology ensured that serial sectioning of paraffin-embedded tumors started directly at the microtumor borders (Figure 1B, Materials and Methods) without the need to search the tumors during serial sectioning in the paraffin block. This approach was crucial for the rapid histological analysis of microtumors.

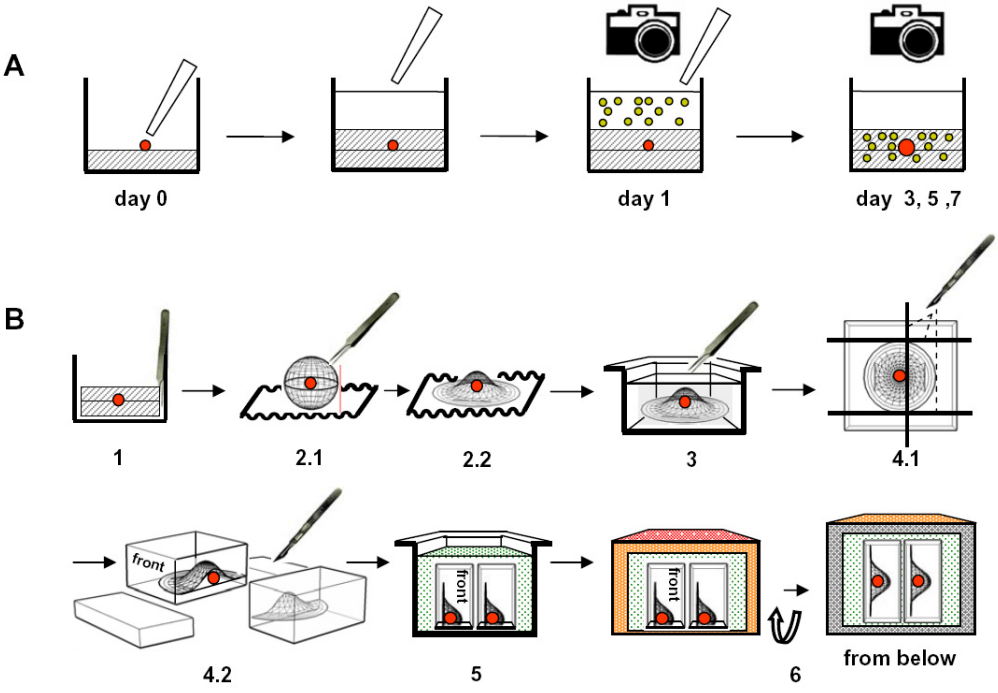

Figure 1. Microtumor generation, CTL treatment and processing for histological analysis. (A) Microtumors were generated on day 0 by embedding of tumor cells between two layers of collagen type I in a 96 well plate well and subsequently covered with medium. In order to study the in situ response of human tumor-epitope specific CTLs against human microtumors, CTLs were added to the microtumor cultures on day 1. On day 3, 5 and 7 tumor size was quantified and supernatant was stored for cytokine analysis. (B) For histological analysis, microtumors in collagen were formalin fixed. The microtumor containing collagen clot was separated from the well wall with a watchmaker's forceps (1) and transferred onto a tissue paper to absorb excessive formalin (2). The shape of the cylindrical collagen clot (1) changed upon transfer to a round (2.1) and after fluid drainage to a bell shape (2.2). The collagen clot was stabilized by embedding into liquid agar at 65°C in a tissue mold (3). After solidification at room temperature, the agar block was dissected along the microtumor border and then laterally trimmed (4.1, 4.2). Several microtumor containing segments were placed with the microtumor cutting edges facing downwards and in perpendicular position into new liquid agar (5). After solidification, the agar block was paraffin-embedded with the tumor cutting edges at the bottom (6) and serial sections were made.

We generated microtumors from the tumor cell lines BB65-RCC, MDA-MB 231, 518A2 and MCF-7. Tumor cells of all cell lines in monolayer cultures had a spindle shaped morphology (except MCF7, which had an epitheloid morphology) (data not shown). Microtumors in culture were clearly visible by light microscopy (Figure 2A). Histology revealed compact 3D microtumors with distinct morphologies already on day 3 of culture (Figure 2B, C).

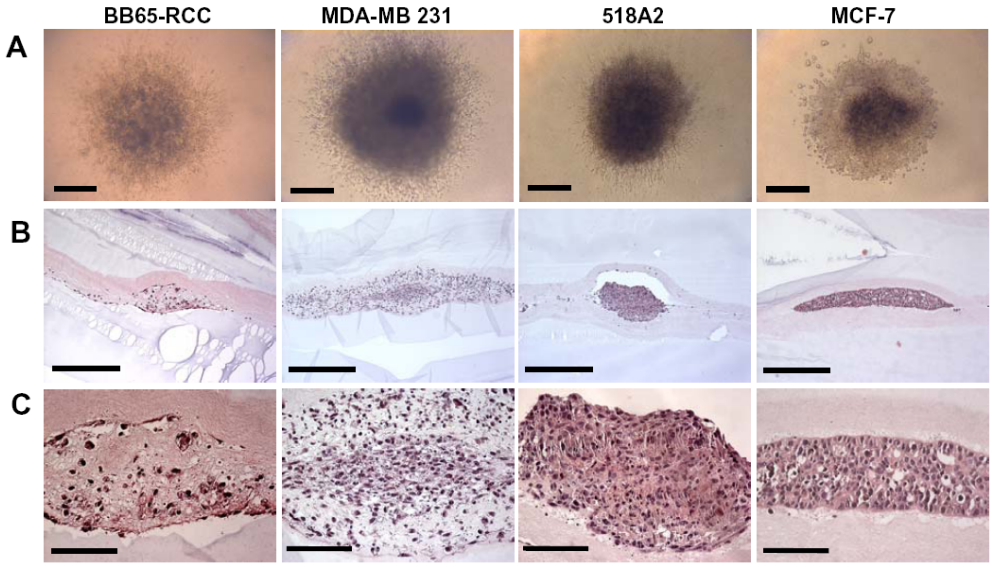

Figure 2. Microtumors are already 3D on day 3 of in vitro culture. Depicted are microtumors derived from the cell lines BB65-RCC, MDA-MB 231, 518A2 and MCF-7 after 3 days of in vitro culture. (A) microtumor in culture; (B, C) H&E stainings of central longitudinal cross sections of microtumors; bar 500 µm (A,B) or 100 µm (C).

Microtumors of different cell lines have distinct histologies

The validity of the generated microtumors as surrogates for clinical cancers was determined by histological and immunohistochemical analysis on day 7. Microtumors strongly resembled histopathological (Figure 3B) and immunohistochemical features (Figure 3C) of the analogous clinical cancers from which the tumor cell lines were derived (Figure 3A). The tumor cell line BB65-RCC was derived from a primary human kidney tumor defined as a clear cell carcinoma, grade II to III (24). BB65-RCC microtumors (Figure 3B) showed the typical morphology of clear cells similar to a primary intermediately differentiated renal clear cell carcinoma (Figure 3A). BB65-RCC microtumors stained characteristically for CD10, vimentin and reticulin fibers (Figure 3C) which was compatible with a renal clear cell carcinoma (36). The tumor cell line MDA-MB 231 was derived from the pleural effusion of a patient with a low differentiated human adenocarcinoma of the breast (27). MDA-MB 231 microtumors (Figure 3B) contained spindle formed cells without orientation similar to a primary breast spindle cell carcinoma (Figure 3A). Immunohistochemistry revealed - like in primary spindle cell carcinomas (37-39) - the simultaneous presence of the epithelial markers keratin and EMA and the mesenchymal marker Vimentin (Figure 3C). Accordingly, MDA-MB 231 microtumors were also estrogen receptor negative

(data not shown). Thus, MDA-MB 231 might be derived from a spindle cell component of the primary tumor. The tumor cell line 518A2 was derived from a human metastasized melanoma (28).

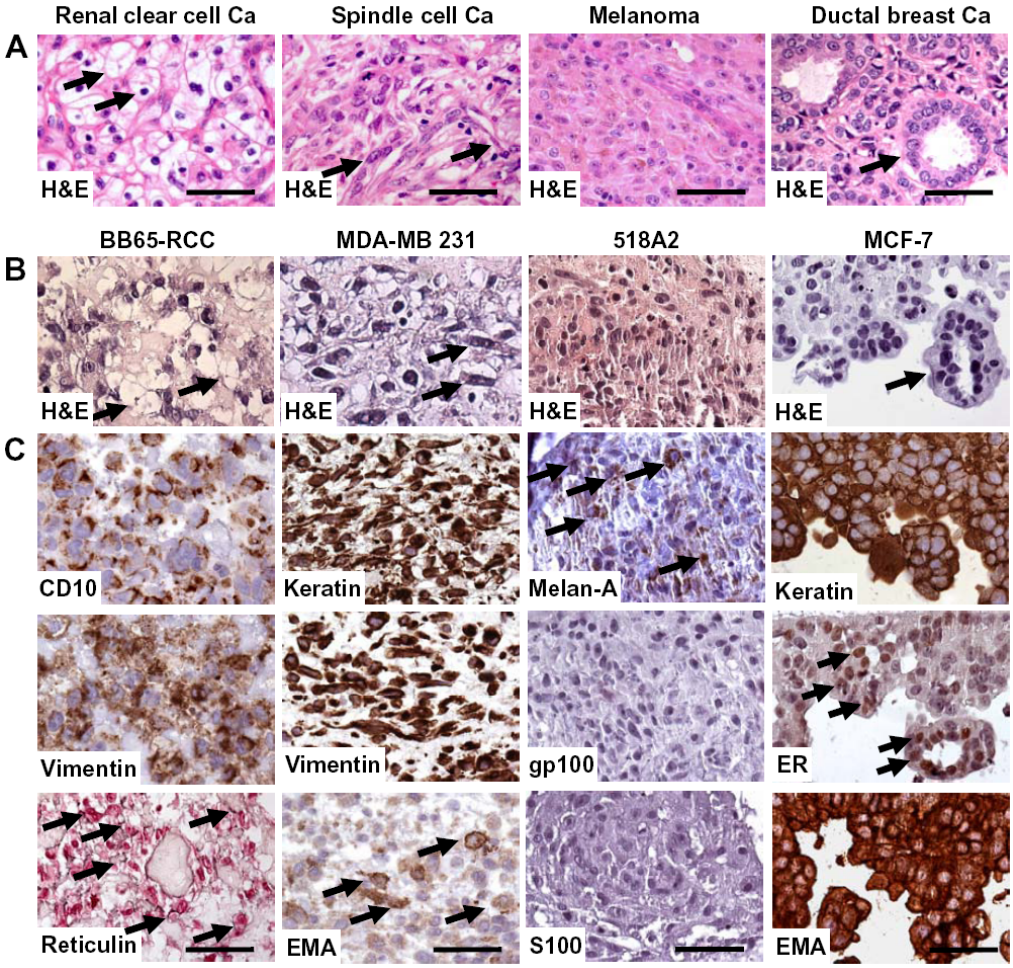

Figure 3. Microtumors have morphological features of primary tumors. Histopathological features (H&E stainings) of primary tumors (A) are resembled by microtumors generated from various cancer cell lines after 7 days of in vitro growth (B). Important characteristics are: clear cells in renal cell carcinoma (arrowheads), spindle formed cells without orientation in spindle cell carcinoma (arrowheads), sheets of atypical melanocytes in melanoma (dense growth pattern) and acinus structures in ductal breast cancer (arrowheads). (C) The in vitro generated microtumors resembled characteristic immunohistochemical staining patterns of the corresponding clinical cancers. Arrowheads indicate: extracellular reticulin, cytoplasmatic staining for Melan-A and nuclear staining for estrogen receptor (ER). Bar, 100 µm.

518A2 microtumors (Figure 3B) showed sheets of cells similar to a primary melanoma (Figure 3A). The positivity for only one (Melan A) of the three tested melanocytic antigens (Melan A, gp100, S100; Figure 3C) is in accordance with the strong heterogeneity of staining mostly observed in individual primary melanomas (8). The tumor cell line MCF-7 was derived from the pleural effusion of a human mammary adenocarcinoma with ductal structures (26). MCF-7 microtumors showed acinus like

structures similar to a primary ductal carcinoma of the breast (Fig 3A). Positivity for keratin and EMA (Figure 3C) and negativity for vimentin (data not shown) supported the epithelial origin of this tumor. Moreover, MCF-microtumors were positive for estrogen receptor (Figure 3C) which was compatible with ductal breast carcinoma (40). Overall, microtumors originating from different cancer cell lines show tumor entity-specific features.

Microtumors contain distinct niches of growth

Tumor growth is the result of a positive balance between tumor cell proliferation and cell death. Ki-67 staining revealed in all microtumors a similarly heterogeneous growth pattern as in primary tumors with a most pronounced proliferative activity at the borders of all investigated tumors (Figure 4A). In order to find indications for central necrosis as in primary tumors in vivo, we prolonged the culture period of MDA-MB 231 and MCF-7 microtumors from 7 days to 14 days. Only MCF-7 microtumors showed a central necrosis (Figure 4B), while MDA-MB 231 microtumors did not contain necrotic areas (data not shown).

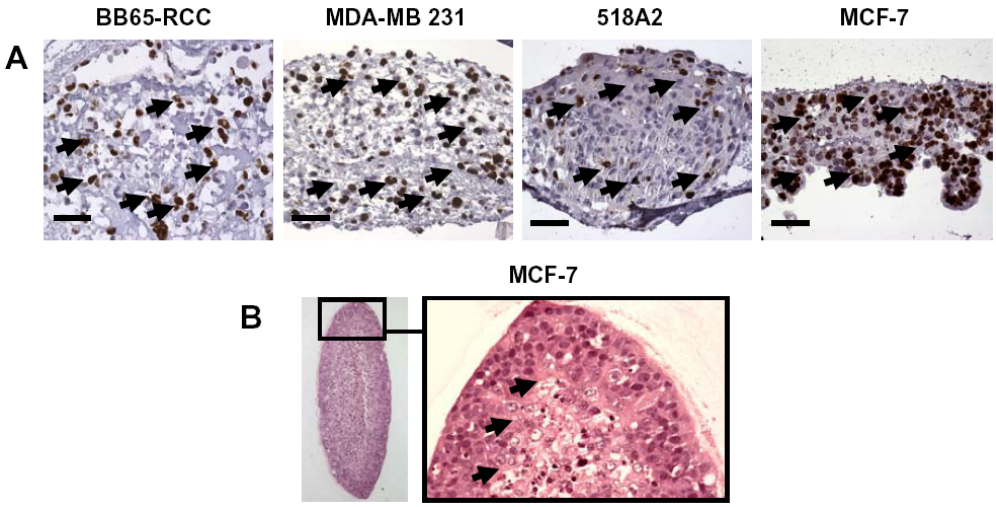

Figure 4. Growth activity and central necrosis in vitro and tumor morphology in vivo. (A) Ki67 stainings on BB65-RCC, MDA-MB 231, 518A2 and MCF-7 microtumors on day 7 show heterogeneous growth activities throughout the tumors, most pronounced in the tumor periphery. Arrowheads indicate Ki67 positive cells; bar, 50 µm. (B) MCF-7 microtumors on day 14 are centrally necrotic. bar, 250 µm; insert: bar, 50 µm. Arrowheads indicate the transition from viable to necrotic areas.

Tumor infiltration, cytokine release and tumor growth inhibition by human CTLs

Next, we studied the applicability of the 3D microtumors as in vitro tumor surrogates for cancer immunotherapy studies. The HLA-A2 restricted mHags HA-1 and H-Y (25) were used as model tumor antigens. Previous genomic typing and mRNA expression analysis had revealed a differential expression of the mHags HA-1 and H-Y by the HLA-A2+ tumor cell lines used in this study. MHag expression was associated with antigen-specific tumor cell killing by HA-1 or H-Y specific CTLs (HA-1 or H-Y CTLs) in a standard 4h ^{51}Cr-release assay (24,30,41). Microtumors were generated from BB65-RCC, MDA-MB-231, 518A2 and MCF-7 tumor cells on day 0 and HA-1 CTLs, H-Y CTLs or medium only were added on day 1. On day 3, 3D microtumors were fixed with paraformaldehyde and subjected to serial

sections. CD8 immunohistochemistry on the serial sections revealed microtumor infiltration by HA-1 and H-Y CTLs both in microtumors positive and negative for the relevant antigen (Figure 5). Microtumor destruction on day 3 by HA-1 and H-Y CTLs was specific for the presence of the relevant antigen on the microtumors (Figure 5).

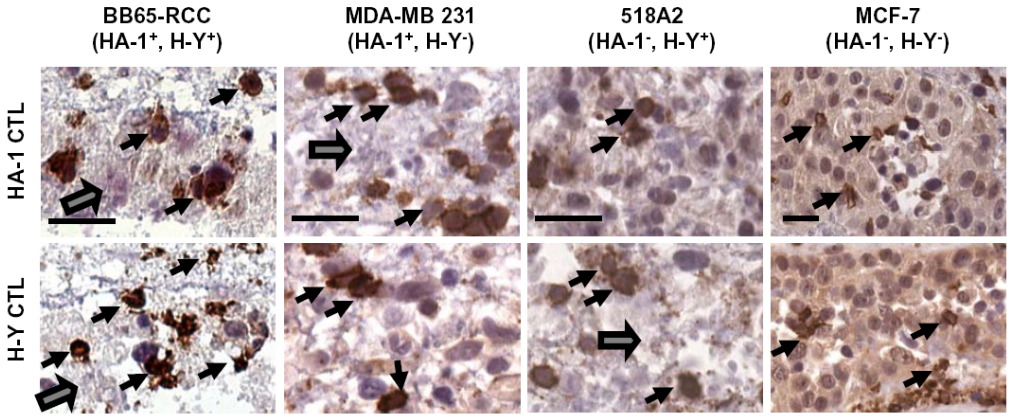

Figure 5. Tumor antigen specific CTLs infiltrate and eradicate microtumors. The different tumor cell lines show a differential expression of the mHags HA-1 and H-Y. Microtumors generated from these tumor cell lines were coincubated with HA-1 and H-Y CTLs. After 3 days, CD8 staining on serial sections of these microtumors revealed that HA-1 CTLs (upper row) and H-Y CTLs (lower row) had infiltrated into the microtumors (closed arrowheads: CD8+ CTLs). Interaction of HA-1 CTLs and H-Y CTLs with microtumors expressing the specific mHags induced tumor cell killing and cell debris (open arrowheads); bar, 50 μm.

Next, the kinetics of cytokine release and tumor growth inhibition mediated by mHag CTLs was studied. Interferon-γ (IFN-γ) was quantified in the supernatant of CTL treated MDA-MB-231 and 518A2 microtumors on day 3, 5 and 7. IFN-γ was only detectable in response to CTLs specific for mHags expressed by the microtumors. IFN-γ levels were maximal on day 3 and subsequently declined (Figure 6A). To determine tumor growth inhibition in response to treatment, 3D microtumors were photographed on day 1, 3, 5 and 7, the 2 maximal orthogonal microtumor radii were measured on these individual photographs and the tumor areas were calculated. HA-1 CTLs only inhibited the growth of the HA-1^+ microtumors MDA-MB 231 (Figure 6B, upper row) and BB65-RCC (data not shown), while H-Y CTLs only inhibited the growth of the male derived H-Y^+ microtumors 518A2 (Figure 6B, lower row) and BB65-RCC (data not shown). Growth of microtumors not expressing the relevant mHag targeted by the CTLs was not affected even at high effector to target (E/T) ratios of 15:1. HA-1 CTLs induced dose-dependent anti-tumor effects (Figure 6C) with reduced MDA-MB 231 microtumor progression at a 5:1 E/T ratio and total growth inhibition at a 15:1 E/T ratio. Overall, 3D microtumors can be used to determine tumor infiltration by CTL, direct cellular effects of CTLs, soluble factors and tumor growth inhibition in response to CTLs.

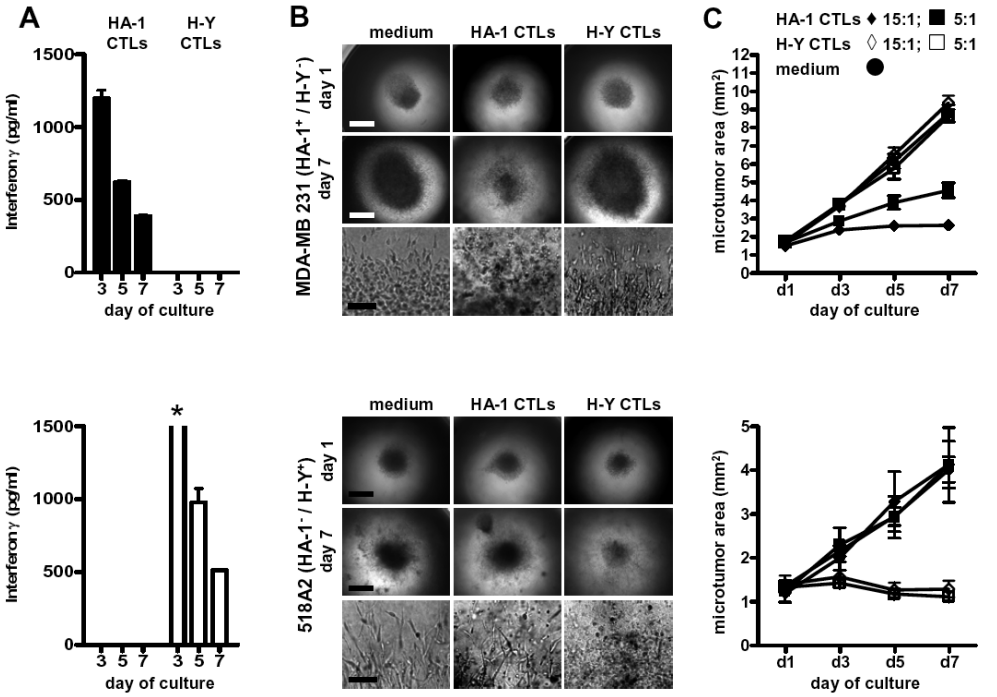

Figure 6. Monitoring of anti-tumor responses mediated by tumor antigen specific CTLs. MDA-MB 231 (upper row) and 518A2 (lower row) microtumors were used. (A) IFN-γ in the supernatant of mHag HA-1 or H-Y CTL treated microtumors. Bars correspond to mean +/- SEM (4 measurements per sample). Star: off-scale measurement. (B) Microtumors on day 1 (top row) and on day 7 (middle and bottom row) after medium or mHag HA-1 or H-Y CTL treatment (effector to target ratio: 15:1); top and middle row: bar, 1 mm; bottom row: bar, 100 µm. Intact tumors on day 7 (bottom row) contain spindle shaped tumor cells; destroyed tumors contain mainly cell debris. (C) Microtumor growth after medium or mHag HA-1 or H-Y CTL treatment (effector to target ratio: 15:1 or 5:1). Each line represents mean microtumor area +/- SEM (data are pooled from 2 independent experiments resulting in median 3 (range 3-9) microtumors per condition).

DISCUSSION

The development of successful cancer immunotherapies requires tumor models resembling important features of the clinical cancers. Here, we present a novel assay for the integrated in-situ analysis of the efficacy of human tumor-antigen specific T-cells against 3D tumors. In this new in vitro model, 3D tumors of several millimeter diameter can be reproducibly generated in a collagen type I matrix. A newly developed protocol allowed a rapid histological assessment of individual microtumors even as small as 500 µm. Namely, the microtumors were organized within the paraffin block in such a way that serial sectioning of microtumors starts directly at the microtumor border. Our study shows that the 3D microtumors generated from different tumor cell lines have distinct morphologies and closely resemble important histological features of the corresponding clinical cancers. 3D microtumors contained clear cells (BB65-RCC, renal clear cell Ca), formed tumor cell sheets (518A2, melanoma) or showed acinus structures (MCF-7, primary infiltrative ductal breast cancer), which fundamentally differed from the morphologies of most of the used tumor cell lines in monolayer cultures. Also the immunohistochemical staining patterns and the presence of tumor-derived ECM (reticulin for BB65-RCC microtumors) were compatible with the intra- and extracellular proteins expressed by clinical tumors of the corresponding entities. Additionally, the dynamics of growth and cell death resembled the heterogeneity of clinical cancers in our model. Namely, while the proliferative activity in our 3D culture system was most pronounced at the microtumor borders, MCF-7 microtumors grown for 14 days were centrally necrotic, which is an indicator for reduced oxygen levels in the inferior parts of the tumor similar to clinical cancers (5,22). Thus, the in vitro microtumors contain distinct niches with outer proliferative and inner less viable tumor regions. The heterogeneous tumor antigen expression in our model is an additional important feature highly important for the correct evaluation of cancer immunotherapies. Namely, despite many tumors are considered positive for tumor associated antigens (TAAs), e.g. melanocyte differentiation (e.g. MelanA/MART-1 or gp100) (8) or for cancer testis antigens (e.g. MAGE–1 or NY-ESO-1) (9,10), a considerable proportion of tumor cells in clinical tumors are TAA negative. Consequently, TAA specific immunotherapies often only deplete the TAA positive tumor cells in vivo without preventing the overall tumor progression (42). The heterogeneous target antigen expression of clinical tumors is well resembled in our model by the differential cellular expression of e.g. MelanA in 518A2 melanoma or of EMA in MDA-MB 231 breast cancer microtumors. Overall, the presented 3D culture system creates several histological features, immunohistochemical staining patterns, distinct tumor growth compartments and heterogeneous protein expression with strong similarities with clinical cancers. Evidently, the 3D tumors in our culture system are not vascularized. Therefore, the described 3D tumors can only serve as models for avascular tumor stages or micrometastases.

We applied these 3D tumors to immunotherapy with antigen-specific CTLs. In contrast to previously described in vitro tumor models (21,22), individual 3D tumors are generated per well in our model. Thereby, 3D tumors can be individually monitored and assessed for several features after T-cell treatment, such as CTL infiltration into tumor tissue, tumor cell killing, cytokine release and tumor growth inhibition. Immunohistochemical analysis of the 3D tumors after addition of T-cells revealed T-cell infiltration by HA-1 and H-Y specific CTLs in both mHag positive and negative tumors. Only the infiltration of HA-1 or H-Y positive but not of negative tumors by HA-1 or H-Y CTLs, respectively, was associated with destruction of tumor cells. These antigen-specific cytotoxic effects in situ were associated with the antigen-specific release of interferon gamma in the supernatant. Additional studies are needed to test whether the collagen matrix is generally sufficiently permeable to monitor soluble

factors in the supernatant. Finally, the optically transparent collagen type I matrix facilitated growth monitoring of individual tumors by repetitive photographic tumor size quantification at various time points. Tumor growth monitoring revealed that also mHag CTL mediated tumor growth inhibition was strictly antigen-specific in this assay.

The presented assay is a highly versatile platform to test the anti-tumor efficacy of various T-cell subsets, NK-cells or antibodies or to investigate the impact of stromal components on tumor infiltration by immune cells (2-4,43). Nevertheless, several features of the presented 3D tumor model still need further improvements. First, microtumor generation using very small volumes of tumor cell suspensions requires serious training. Automatic injector systems, as previously applied in the context of tuberculosis studies (44), might be used to place the tumor droplets via a fine needle into the collagen matrix and to generate equally shaped tumors at high-throughput level. Second, accurate quantification of CTL infiltration into tumors requires CD8 staining on many parallel sections per microtumor. The analysis of tumor infiltration might be facilitated by usage of fluorescently marked tumor and T-cells and subsequent analysis by confocal laser microscopy without previous paraffin embedding. Finally, determination of tumor growth based on only 2D photographies is not entirely comprehensive, because it does not consider the tumor size on the vertical axis. Usage of luciferase transfected tumor cells and subsequent quantification of the tumor load by luminscence imaging (45) may further improve the accuracy of tumor size quantification

Conclusion

The presented in vitro culture system provides an unlimited source of experimental solid tumors of different entities and with defined properties, such as the presence or absence of the tumor target molecules. Human tumors engineered in 3D scaffolds allow monitoring of multiple parameters in response to treatment. Thereby, these 3D tumors can provide an integrated view on the mechanisms and the anti-tumor efficacy of cellular immunotherapy in situ.

ACKNOWLEDGEMENTS

The authors thank Dr. Machteld Oudshoorn, Dr. Marieke Hoeve and Dr. Kam-Wing Ling for critical reading of the manuscript and Dr. P. Schrier and Dr. B. Van den Eynde for providing tumor cell lines.

REFERENCES

1. Klebanoff, C. A., N. Acquavella, Z. Yu, and N. P. Restifo. 2011. Therapeutic cancer vaccines: are we there yet? *Immunol.Rev.* 239:27-44.
2. Yang, Q., S. Goding, M. Hagenaars, T. Carlos, P. Albertsson, P. Kuppen, U. Nannmark, M. E. Hokland, and P. H. Basse. 2006. Morphological appearance, content of extracellular matrix and vascular density of lung metastases predicts permissiveness to infiltration by adoptively transferred natural killer and T cells. *Cancer Immunol Immunother.* 55:699-707.
3. Kuppen, P. J., M. M. van der Eb, L. E. Jonges, M. Hagenaars, M. E. Hokland, U. Nannmark, R. H. Goldfarb, P. H. Basse, G. J. Fleuren, R. C. Hoeben, and C. J. van de Velde. 2001. Tumor structure and extracellular matrix as a possible barrier for therapeutic approaches using immune cells or adenoviruses in colorectal cancer. *Histochem.Cell Biol.* 115:67-72.
4. Singh, S., S. R. Ross, M. Acena, D. A. Rowley, and H. Schreiber. 1992. Stroma is critical for preventing or permitting immunological destruction of antigenic cancer cells. *J.Exp.Med.* 175:139-146.
5. Sutherland, R. 1988. Cell and environment interactions in tumor microregions: the multicell spheroid model. *Science* 240:177-184.

6. Ghosh, S., G. Spagnoli, I. Martin, S. Ploegert, P. Demougin, M. Heberer, and A. Reschner. 2006. Three-dimensional culture of melanoma cells profoundly affects gene expression profile: a high density oligonucleotide array study. *J Cell Physiol* 204:522-531.
7. Feder-Mengus, C., S. Ghosh, W. P. Weber, S. Wyler, P. Zajac, L. Terracciano, D. Oertli, M. Heberer, I. Martin, G. C. Spagnoli, and A. Reschner. 2007. Multiple mechanisms underlie defective recognition of melanoma cells cultured in three-dimensional architectures by antigen-specific cytotoxic T lymphocytes. *Br.J.Cancer* 96:1072-1082.
8. de Vries, T. J., M. Smeets, R. de Graaf, K. Hou-Jensen, E. B. Brocker, N. Renard, A. M. Eggermont, G. N. van Muijen, and D. J. Ruiter. 2001. Expression of gp100, MART-1, tyrosinase, and S100 in paraffin-embedded primary melanomas and locoregional, lymph node, and visceral metastases: implications for diagnosis and immunotherapy. A study conducted by the EORTC Melanoma Cooperative Group. *J.Pathol.* 193:13-20.
9. Jungbluth, A. A., E. Stockert, Y. T. Chen, D. Kolb, K. Iversen, K. Coplan, B. Williamson, N. Altorki, K. J. Busam, and L. J. Old. 2000. Monoclonal antibody MA454 reveals a heterogeneous expression pattern of MAGE-1 antigen in formalin-fixed paraffin embedded lung tumours. *Br.J.Cancer* 83:493-497.
10. Jungbluth, A. A., Y. T. Chen, E. Stockert, K. J. Busam, D. Kolb, K. Iversen, K. Coplan, B. Williamson, N. Altorki, and L. J. Old. 2001. Immunohistochemical analysis of NY-ESO-1 antigen expression in normal and malignant human tissues. *Int.J.Cancer* 92:856-860.
11. Waleh, N., M. Brody, M. Knapp, H. Mendonca, E. Lord, C. Koch, K. Laderoute, and R. Sutherland. 1995. Mapping of the vascular endothelial growth factor-producing hypoxic cells in multicellular tumor spheroids using a hypoxia-specific marker. *Cancer Res* 55:6222-6226.
12. Lin, S. C., C. W. Chien, J. C. Lee, Y. C. Yeh, K. F. Hsu, Y. Y. Lai, S. C. Lin, and S. J. Tsai. 2011. Suppression of dual-specificity phosphatase-2 by hypoxia increases chemoresistance and malignancy in human cancer cells. *J.Clin.Invest* 121:1905-1916.
13. Bao, Q. and R. C. Hughes. 1999. Galectin-3 and polarized growth within collagen gels of wild-type and ricin-resistant MDCK renal epithelial cells. *Glycobiology* 9:489-495.
14. Cukierman, E., R. Pankov, D. R. Stevens, and K. M. Yamada. 2001. Taking cell-matrix adhesions to the third dimension. *Science* 294:1708-1712.
15. Zegers, M. M., L. E. O'Brien, W. Yu, A. Datta, and K. E. Mostov. 2003. Epithelial polarity and tubulogenesis in vitro. *Trends Cell Biol.* 13:169-176.
16. Clark, E. A., W. G. King, J. S. Brugge, M. Symons, and R. O. Hynes. 1998. Integrin-mediated signals regulated by members of the rho family of GTPases. *J.Cell Biol.* 142:573-586.
17. Zahir, N. and V. M. Weaver. 2004. Death in the third dimension: apoptosis regulation and tissue architecture. *Curr.Opin.Genet.Dev.* 14:71-80.
18. Desoize, B. and J. Jardillier. 2000. Multicellular resistance: a paradigm for clinical resistance? *Crit Rev Oncol Hematol* 36:193-207.
19. Pampaloni, F., E. G. Reynaud, and E. H. Stelzer. 2007. The third dimension bridges the gap between cell culture and live tissue. *Nat.Rev.Mol.Cell Biol.* 8(10):839-45
20. Ivascu, A. and M. Kubbies. 2006. Rapid generation of single-tumor spheroids for high-throughput cell function and toxicity analysis. *J.Biomol.Screen.* 11:922-932.
21. Lee, G. Y., P. A. Kenny, E. H. Lee, and M. J. Bissell. 2007. Three-dimensional culture models of normal and malignant breast epithelial cells. *Nat.Methods* 4:359-365.
22. Fischbach, C., R. Chen, T. Matsumoto, T. Schmelzle, J. S. Brugge, P. J. Polverini, and D. J. Mooney. 2007. Engineering tumors with 3D scaffolds. *Nat.Methods* 4:855-860.
23. Wei, W., B. Miller, and R. Gutierrez. 1997. Inhibition of tumor growth by peptide specific cytotoxic T lymphocytes in a thrree-dimensional collagen matrix. *J Immunol Methods* 200:47-54.
24. Hambach, L., M. Vermeij, A. Buser, Z. Aghai, K. T. van der, and E. Goulmy. 2008. Targeting a single mismatched minor histocompatibility antigen with tumor-restricted expression eradicates human solid tumors. *Blood* 112:1844-1852.
25. Hambach, L. and E. Goulmy. 2005. Immunotherapy of cancer through targeting of minor histocompatibility antigens. *Curr Opin Immunol* 17:202-210.
26. Soule, H. D., J. Vazguez, A. Long, S. Albert, and M. Brennan. 1973. A human cell line from a pleural effusion derived from a breast carcinoma. *J.Natl.Cancer Inst.* 51:1409-1416.
27. Cailleau, R., R. Young, M. Olive, and W. J. Reeves, Jr. 1974. Breast tumor cell lines from pleural effusions. *J.Natl.Cancer Inst.* 53:661-674.

28. Versteeg, R., I. A. Noordermeer, M. Kruse-Wolters, D. J. Ruiter, and P. I. Schrier. 1988. c-myc down-regulates class I HLA expression in human melanomas. *EMBO J.* 7:1023-1029.
29. Spierings, E., J. Drabbels, M. Hendriks, J. Pool, M. Spruyt-Gerritse, F. Claas, and E. Goulmy. 2006. A uniform genomic minor histocompatibility antigen typing methodology and database designed to facilitate clinical applications. *PLoS.ONE.* 1:e42.
30. Klein, C., M. Wilke, J. Pool, C. Vermeulen, E. Blokland, E. Burghart, S. Krostina, N. Wendler, B. Passlick, G. Riethmueller, and E. Goulmy. 2002. The hematopoietic system-specific minor histocompatibility antigen HA-1 shows aberrant expression in epithelial cancer cells. *J Exp Med* 196:359-368.
31. Mutis, T., R. Verdijk, E. Schrama, B. Esendam, A. Brand, and E. Goulmy. 1999. Feasibility of immunotherapy of relapsed leukemia with ex vivo-generated cytotoxic T lymphocytes specific for hematopoietic system-restricted minor histocompatibility antigens. *Blood* 93:2336-2341.
32. de Bueger, M., A. Bakker, J. van Rood, F. van der Woude, and E. Goulmy. 1992. Tissue distribution of human minor histocompatibility antigens. Ubiquitous versus restricted tissue distribution indicated heterogenity among human cytotoxic T lymphocyte-defined non-MHC antigens. *J Immunol* 149 (5):1788-1794.
33. Gomorri, G. 1937. Silver impregnation of reticulin in paraffin sections. Am J Pathol 13: 993-1002.
34. Russo, J., H. D. Soule, C. McGrath, and M. A. Rich. 1976. Reexpression of the original tumor pattern by a human breast carcinoma cell line (MCF-7) in sponge culture. *J.Natl.Cancer Inst.* 56:279-282.
35. Fata, J. E., Z. Werb, and M. J. Bissell. 2004. Regulation of mammary gland branching morphogenesis by the extracellular matrix and its remodeling enzymes. *Breast Cancer Res.* 6:1-11.
36. Skinnider, B. F. and M. B. Amin. 2005. An immunohistochemical approach to the differential diagnosis of renal tumors. *Semin.Diagn.Pathol.* 22:51-68.
37. Maemura, M., Y. Iino, T. Oyama, T. Hikino, T. Yokoe, H. Takei, J. Horiguchi, S. Ohwada, T. Nakajima, and Y. Morishita. 1997. Spindle cell carcinoma of the breast. *Jpn.J.Clin.Oncol.* 27:46-50.
38. Carter, M. R., J. L. Hornick, S. Lester, and C. D. Fletcher. 2006. Spindle cell (sarcomatoid) carcinoma of the breast: a clinicopathologic and immunohistochemical analysis of 29 cases. *Am.J.Surg.Pathol.* 30:300-309.
39. Wargotz, E. S., P. H. Deos, and H. J. Norris. 1989. Metaplastic carcinomas of the breast. II. Spindle cell carcinoma. *Hum.Pathol.* 20:732-740.
40. Steinman, S., J. Wang, P. Bourne, Q. Yang, and P. Tang. 2007. Expression of cytokeratin markers, ER-alpha, PR, HER-2/neu, and EGFR in pure ductal carcinoma in situ (DCIS) and DCIS with co-existing invasive ductal carcinoma (IDC) of the breast. *Ann.Clin.Lab Sci.* 37:127-134.
41. Hambach, L., K. W. Ling, J. Pool, Z. Aghai, E. Blokland, H. J. Tanke, J. A. Bruijn, H. Halfwerk, H. van Boven, B. Wieles, and E. Goulmy. 2009. Hypomethylating drugs convert HA-1-negative solid tumors into targets for stem cell-based immunotherapy. *Blood* 113:2715-2722.
42. Mackensen, A., N. Meidenbauer, S. Vogl, M. Laumer, J. Berger, and R. Andreesen. 2006. Phase I study of adoptive T-cell therapy using antigen-specific CD8+ T cells for the treatment of patients with metastatic melanoma. *J.Clin.Oncol.* 24:5060-5069.
43. Netti, P. A., D. A. Berk, M. A. Swartz, A. J. Grodzinsky, and R. K. Jain. 2000. Role of extracellular matrix assembly in interstitial transport in solid tumors. *Cancer Res.* 60:2497-2503.
44. Carvalho, R., J. de Sonneville, O. W. Stockhammer, N. D. Savage, W. J. Veneman, T. H. Ottenhoff, R. P. Dirks, A. H. Meijer, and H. P. Spaink. 2011. A high-throughput screen for tuberculosis progression. *PLoS.ONE.* 6:e16779.
45. Palm, D., K. Lang, B. Brandt, K. S. Zaenker, and F. Entschladen. 2005. In vitro and in vivo imaging of cell migration: two interdepending methods to unravel metastasis formation. *Semin.Cancer Biol.* 15:396-404.